Biaxially strained germanium crossbeam with a high-quality optical cavity for on-chip laser applications

Jung, Yongduck; Kim, Youngmin; Burt, Daniel; Joo, Hyo-Jun; Kang, Dong-Ho; Luo, Manlin; Chen, Melvina; Lin, Zhang; Tan, Chuan Seng; Nam, Donguk

2021

Jung, Y., Kim, Y., Burt, D., Joo, H., Kang, D., Luo, M., Chen, M., Lin, Z., Tan, C. S. & Nam, D. (2021). Biaxially strained germanium crossbeam with a high-quality optical cavity for on-chip laser applications. Optics Express, 29(10), 14174-14181. https://dx.doi.org/10.1364/OE.417330

https://hdl.handle.net/10356/148836

https://doi.org/10.1364/OE.417330

Research Article | Vol. 29, No. 10 / 10 May 2021 / Optics Express 14174
Optics EXPRESS

Biaxially strained germanium crossbeam with a high-quality optical cavity for on-chip laser applications

YONGDUCK JUNG,[1,2] YOUNGMIN KIM,[1,2] DANIEL BURT,[1] HYO-JUN JOO,[1] DONG-HO KANG,[1] MANLIN LUO,[1] MELVINA CHEN,[1] LIN ZHANG,[1] CHUAN SENG TAN,[1] AND DONGUK NAM[1,*]

[1]*School of Electrical and Electronic Engineering, Nanyang Technological University, 50 Nanyang Avenue, Singapore 639798, Singapore*
[2]*These authors contributed equally to this work*
[*]*dnam@ntu.edu.sg*

Abstract: The creation of CMOS compatible light sources is an important step for the realization of electronic-photonic integrated circuits. An efficient CMOS-compatible light source is considered the final missing component towards achieving this goal. In this work, we present a novel crossbeam structure with an embedded optical cavity that allows both a relatively high and fairly uniform biaxial strain of ~0.9% in addition to a high-quality factor of >4,000 simultaneously. The induced biaxial strain in the crossbeam structure can be conveniently tuned by varying geometrical factors that can be defined by conventional lithography. Comprehensive photoluminescence measurements and analyses confirmed that optical gain can be significantly improved via the combined effect of low temperature and high strain, which is supported by a three-fold reduction of the full width at half maximum of a cavity resonance at ~1,940 nm. Our demonstration opens up the possibility of further improving the performance of germanium lasers by harnessing geometrically amplified biaxial strain.

1. Introduction

During the last few years, there have been relentless efforts to transform germanium (Ge) into a direct bandgap material for high-performance on-chip laser applications, and ultimately for the realization of photonic-integrated circuits [1–24]. The leading forms of band engineering for achieving on-chip lasing from Ge include uniaxial [4,5,11,12,25] and biaxial strain [8,16,21,22,26] engineering, both of which lower the direct conduction Γ valley faster than the indirect L valleys. Among a large variety of strain engineering platforms (including the use of external stressor layers [3,8,22]), the geometrical strain amplification technique [4,5,27] has been widely used particularly for uniaxial strain engineering. The formation of a substantially large uniaxial strain of up to a few percent enabled by the geometrical amplification technique has led to the successful development of Ge lasers [28,29]. Notably, a direct bandgap has been achieved in Ref. [29] by inducing a 5.9% uniaxial strain. Such a large uniaxial strain narrows the bandgap severely and shifts the emission wavelength beyond >3.5 μm. Despite new possibilities towards free-space mid-infrared sensing applications [28], the mid-infrared emission renders it impossible for the uniaxially strained Ge lasers to be employed for optical board-to-board communication applications owing to the opaque nature of silica-based optical fibers [30].

Biaxial strain has a unique advantage in that the bandgap narrowing by biaxial strain is substantially smaller compared to the uniaxial case. In fact, the direct bandgap that can be achieved by >1.67% biaxial strain allows the emission wavelength to be located ~2 μm [31], thus enabling biaxially strained Ge lasers to be employed for fiber-based optical communications. Recently, by using the external stressor layer technique, biaxially strained Ge microdisk lasers

#417330 https://doi.org/10.1364/OE.417330
Journal © 2021 Received 14 Dec 2020; revised 7 Feb 2021; accepted 7 Apr 2021; published 26 Apr 2021

Optics EXPRESS

in a direct bandgap configuration have been demonstrated with an emission wavelength of ~2 μm [32]. However, the use of an external stressor layer requires precise control of the stressor layer thickness, which otherwise could lead to a significant gain broadening owing to strain inhomogeneity within the active gain medium. In addition, the strain level is purely determined by the thickness and the residual stress of the stressor layer, both of which are predetermined at the stage of the wafer bonding [8,24,33]. A few research groups have reported lithographically tunable biaxial strain enabled by the geometrical strain amplification technique [10,17]. Although this technique poses distinctive advantages towards creating biaxially strained Ge lasers in terms of strain homogeneity and tunability, the understanding of the optical gain in such structures remains missing largely owing to the challenges in embedding high-quality optical cavities without disturbing the homogeneous strain distribution.

In this article, we propose a novel crossbeam structure that can achieve a lithographically tunable biaxial strain with embedded distributed Bragg reflector (DBR) mirrors. By employing the geometrical strain amplification technique along two orthogonal axes, we obtain a fairly uniform strain distribution within the gain medium. The DBR mirrors are carefully designed to have a high-quality factor of >4,000 without disturbing the strain homogeneity, allowing for the first demonstration of a high-quality factor optical cavity for geometrically enhanced biaxial strain. Finite-element method (FEM) mechanical simulations along with 2D Raman mapping provides the evidence for the uniformity of the induced biaxial strain. We perform a comprehensive photoluminescence (PL) study to investigate the effect of strain, temperature, and pump power on the optical gain in biaxially strained Ge. Notably, the biaxial strain is further enhanced by lowering the sample temperature because of the thermal expansion coefficient mismatch between Si and Ge [34,35]. The combined effect of temperature and strain is found to have a profound impact on the optical gain, which is evidenced by a three-fold reduction of the full width at half maximum (FWHM) of a cavity resonance at ~1,940 nm. Our work paves the way towards creating biaxially strained Ge lasers for fiber-based optical communication applications.

2. Device fabrication and optical simulation

Figure 1(a) shows a schematic illustration of the detailed fabrication procedure. The device was fabricated using a Ge-on-insulator (GOI) substrate, which was created by using epitaxial growth and a direct wafer bonding technique [28]. An epitaxially grown Ge layer on Si having a 20-nm-thick aluminum oxide (Al_2O_3) layer on top was bonded to a handle Si wafer having a 1-μm-thick thermally grown silicon dioxide (SiO_2) layer. By using wafer backgrinding and tetramethylammonium hydroxide (TMAH) wet etching, the Si carrier wafer was removed, allowing the formation of a GOI wafer. The desired Ge thickness of 300 nm was achieved by a chemical mechanical polishing (CMP) step, which enabled a smooth surface with a surface roughness of <0.3 nm. The threading dislocation density of the as-grown Ge on Si was around 1×10^7 cm^{-2} and after the bonding procedure and removal of defect rich Ge/Si interface it was around 5×10^6 cm^{-2}. The crossbeam structure was defined by electron-beam lithography (EBL) using a positive tone resist ZEP 520A. The pattern was then subsequently transferred using Cl_2- and BCl_3-based inductively coupled plasma (ICP) dry etching. Isotropic wet etching by hydrofluoric (HF) acid was performed to undercut the underlying Al_2O_3 and SiO_2 layers, thus releasing the crossbeam structure. Finally, critical point drying (CPD) [36] allowed for the entire structure to remain suspended by preventing it from adhering to the underlying Si substrate.

Figures 1(b) and 1(c) show top- and tilted-view scanning electron microscopy (SEM) images of a fabricated biaxially strained Ge crossbeam structure. A clear shadow under the central region of the structure is shown due to the suspended nature of the crossbeam structure, which is crucial in amplifying biaxial strain at low temperatures, and thereby enhancing optical gain. This feature will be discussed in section 4 (Fig. 6) of this paper. Upon releasing the patterned crossbeam structure in the HF-based wet etching step, the residual biaxial strain in the entire Ge

Optics EXPRESS

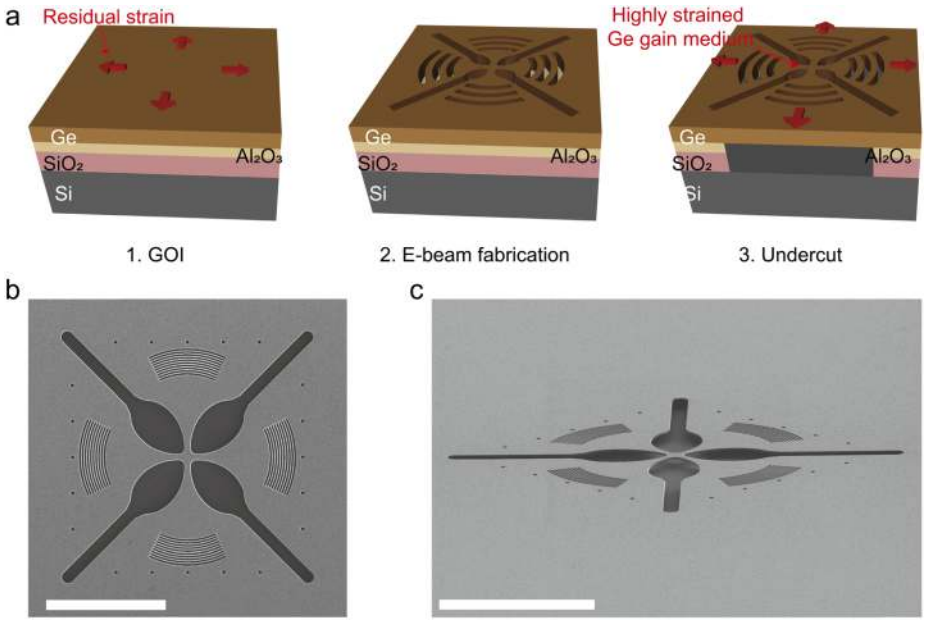

Fig. 1. (a) Schematic illustration of the crossbeam structure fabrication process. (b) Top-view SEM image. Scale bar, 20 μm. (c) Tilted-view SEM image. Scale bar, 20 μm.

layer redistributes and amplifies the strain around the center of the crossbeam structure [27]. The DBR mirrors are integrated at all four sides of the central structure.

Figure 2 shows the simulated electric field distributions for the top and cross-sectional views of our biaxially strained Ge crossbeam structure, which were obtained using 3D finite-domain time-difference (FDTD) simulations. Each DBR mirror consists of 10 air trenches with width and period of 285 nm and 452 nm, respectively. The curvature of circular arcs was carefully designed to achieve a high optical quality factor of >4,000. The crossbeam structure was designed to allow optical fields to overlap with the highly strained gain medium around the center of the crossbeam structure.

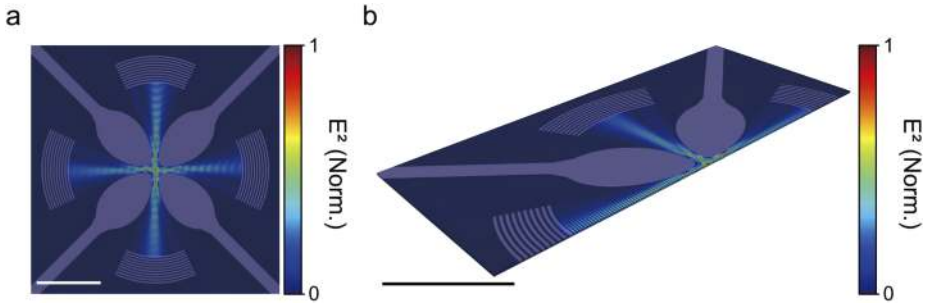

Fig. 2. (a) and (b) Top- and cross-sectional views of simulated electric field distributions in the crossbeam structure that achieves a high-quality factor of >4,000. Scale bar, 10 μm.

3. Structural analysis

To investigate the strain distribution in the crossbeam structure, we employed the FEM simulations using COMSOL Multiphysics. Figures 2(a) and 2(b) show the simulated and measured biaxial

Optics EXPRESS

tensile strain distribution in a typical crossbeam structure, respectively, showing excellent agreement between the two results. The diameter of the central area was 2.42 μm and the minimum width of the neck was 1 μm. For the measured biaxial strain, 2D Raman mapping was conducted by using a 532-nm laser with low power to avoid any heating effects. By using a strain-shift coefficient for biaxial strain [3], we obtained a relatively homogeneous biaxial strain with a maximum value of ~0.86%. The lateral strain variation over a 10-μm length around the center of the gain medium is only ~20% (Fig. 3(c)), verifying a fairly uniform strain distribution in the gain medium that holds the key towards achieving a homogeneous optical gain. The strain homogeneity can be further improved by reducing the central gain medium diameter. The biaxial strain can be further increased by improving the strain homogeneity and by reducing the defect density during the material growth and bonding processes.

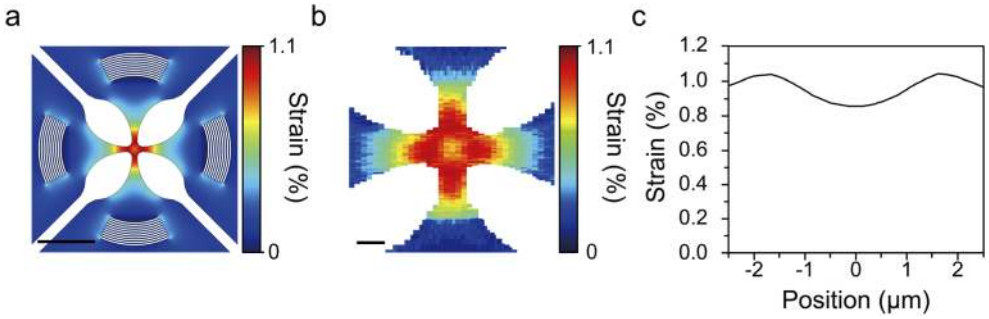

Fig. 3. (a) Simulated biaxial strain distribution in the crossbeam structure. Scale bar, 10 μm. (b) Measured biaxial strain distribution via Raman mapping in the crossbeam structure. Scale bar, 1 μm. (c) Lateral strain variation over a 10-μm length around the center of the gain medium.

4. Optical characterization

To investigate the effect of strain, pump power and temperature on the optical gain in the biaxially strained Ge crossbeam structures, we performed comprehensive PL measurements and analyses. We employed a 1,550-nm-pulsed laser with pulse width and repetition rate of 50 ns and 3 MHz, respectively. The sample was mounted in a cryostat operating at a wide temperature range between 4 K and 300 K. The pump laser was focused onto the sample using a 15x objective lens producing a spot size of around 10 μm, and the signal was collected by the same objective lens and subsequently coupled into a grating which diffracted the spectrum onto a 1D-array extended InGaAs detector with a detection range between 1.4 and 2.1 μm.

Figure 4(a) shows the PL spectra from the crossbeam structures with different strains on a single chip. For comparison, we also present the PL spectrum from an unstrained Ge bulk area, which shows an emission peak at ~1,420 nm. This peak position is consistent with the calculated emission peak at a cryogenic temperature according to the empirical Varshni model [37]. By increasing the biaxial tensile strain from 0.34% (red) to 0.86% (blue), the PL intensity is clearly increased while the peak wavelength position is shifted by ~500 nm. Tensile strain is expected to reduce the energy difference between the direct Γ valley and the indirect L valleys, thus increasing the electron population in the direct Γ valley that contributes to the radiative recombination [38]. The energy gap for the direct radiative optical transition is also reduced at higher tensile strain [22], which is the main reason for such a large peak wavelength shift. The integrated intensity was calculated from the area underneath the whole curve. The FWHM was extracted by utilizing Lorentzian fitting functions. The FWHM of the broad spontaneous emission is also significantly increased at higher strain, and this can be attributed to the strain-induced valence band splitting

Optics EXPRESS

and strain non-homogeneity [39]. The quantitative analysis of the integrated PL intensity as a function of strain shows a three-fold increase of the PL intensity as strain is increased from 0.34% to 0.86% (Fig. 4(b)). Tensile strain is also expected to increase the optical gain because of the increased electron population fraction in the direct Γ valley with respect to the indirect L valleys [35]. The increased optical gain (i.e., reduced optical loss) is also clearly evidenced by the reduced FWHM of the cavity mode at higher strain as shown in Fig. 4(b).

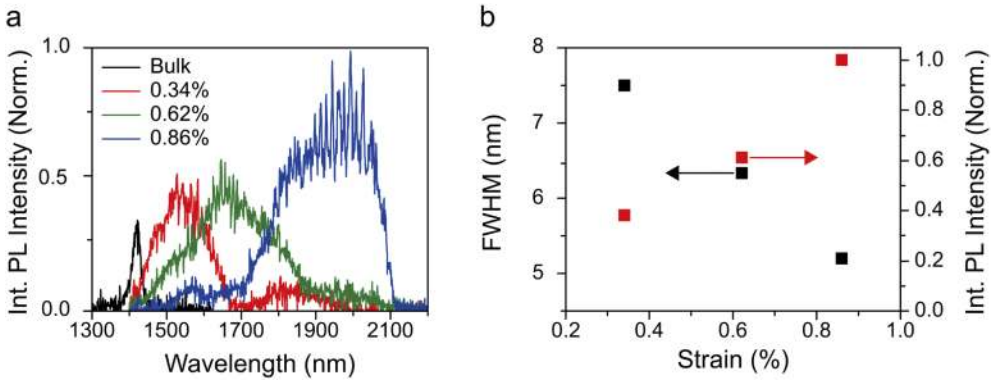

Fig. 4. (a) PL from crossbeam structures with applied biaxial strains of 0.34%, 0.62%, and 0.86%. The measurement temperature was kept at 4 K. (b) The linewidth of the cavity modes and the integrated PL intensity as a function biaxial strain.

Figure 5(a) shows the power dependent PL spectra of the 0.86%-strained Ge crossbeam structure. The measurement temperature was kept at 4 K. At a low pump power of 0.4 kW/cm^2, the PL spectrum shows broad spontaneous emission without any clear, sharp cavity peaks. The peak position of the broad spontaneous emission is at the cut-off of our InGaAs detector (~2,100 nm). At an increased pump power of 2.0 kW/cm^2, sharp cavity modes are clearly observed as the optical loss is compensated by the material gain. It is noteworthy that the peak position of the broad emission is also shifted to a shorter wavelength at ~1,900 nm, and this can be ascribed to the band filling effect. At higher pump power, the excited holes start filling up the second valence band while at low pump power, the pumped holes only occupy the highest valence band [28]. Figure 5(b) presents the linewidth of the cavity mode at ~1,940 nm and the integrated PL intensity as a function of pump power. The FWHM value of the investigated cavity mode is reduced to ~5.2 nm at a pump power of 2.0 kW/cm^2, manifesting the reduced loss at an increased pump power. However, the cavity mode starts broadening as the pump power is further increased. This is in contrast to the previously reported lasing results in uniaxially [28,29] and biaxially [32] strained Ge structures. Also, we did not observe any threshold behavior in the integrated PL intensity as a function of pump power. We believe that the absence of the lasing behavior in our structure is mainly because the induced biaxial strain is not large enough to allow the material gain to overcome the loss in the material and the optical cavity.

Furthermore, temperature-dependent PL measurements were performed at temperatures between 4 K and 300 K (Fig. 6). At 300 K, the PL spectrum only shows a broad spontaneous emission without any cavity modes owing to a large material loss at an elevated temperature. As the temperature is decreased, the cavity modes become sharper and bigger in intensity as shown in Figs. 6(a) and 6(b). The FWHM of the cavity mode at ~1,940 nm is significantly reduced from 15.8 nm to 5.2 nm as the temperature is reduced from 275 K to 4 K, suggesting substantially improved optical gain at lower temperatures. The main factors for this optical gain enhancement at a low temperature include reduced inter-valence band absorption (IVBA) [28] and increased strain at a low temperature [35]. The increase of the induced biaxial strain at a low temperature

Optics EXPRESS

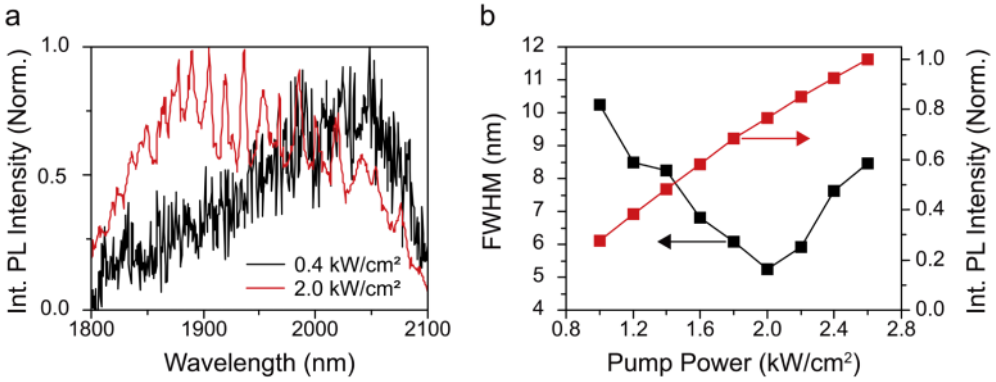

Fig. 5. (a) Pump-power dependence of PL spectra of the 0.86%-strained structure measured at 4 K. (b) The linewidth of the cavity mode at ~1,940 nm and the integrated PL intensity as a function pump power.

is possible in our unique structural geometry where the entire Ge crossbeam structure is fully suspended on air. The weakly distributed residual strain in the Ge layer arises from the thermal expansion coefficient mismatch between Si and Ge [34], and this residual strain is concentrated around the central area of the crossbeam structure [27], thus allowing the accumulation of a large biaxial strain. Since the strength of the strain is temperature-dependent and becomes higher at a low temperature [35], the decrease of the operating temperature increases the strain, which in turn further increases the localized biaxial strain in the central area of the crossbeam structure. This combined effect of temperature and strain has a significant impact on the optical gain, which is evidenced by the three-fold reduction of the FWHM value of a cavity resonance at ~1,940 nm when the temperature is reduced from 275 K to 4 K.

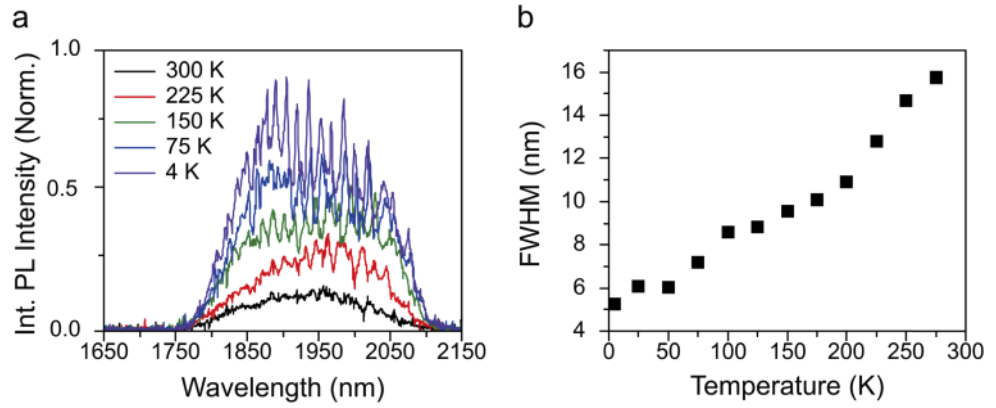

Fig. 6. (a) Temperature dependence of PL spectra of the 0.86%-strained structure measured between 4 K and 300 K. (b) The linewidth of the cavity mode at ~1,940 nm as a function of temperature.

5. Conclusion

We have presented a novel crossbeam structure embedded with DBR mirrors that can simultaneously achieve large biaxial strains and high-quality factors. The geometrical amplification technique employed in this study allowed the creation of multiple structures with distinct strain

Optics EXPRESS

levels on a single chip. Structural analyses via a combination of simulations and experiments confirmed a fairly uniform strain. Comprehensive PL studies were performed to investigate the evolution of cavity modes under different experimental conditions with strain, pump power, and temperature as key variables. Particularly, we observed a three-fold reduction of the FWHM value of the cavity mode by harnessing both lowered material losses and increased biaxial strain at lower operating temperatures. We believe that our new biaxially strained Ge crossbeam design can enable achieving a low-threshold on-chip laser for fiber-based optical communications.

Funding. National Research Foundation Singapore (NRF2018-NRF-ANR009 TIGER, NRF-CRP19-2017-01); Ministry of Education (MOE2018-T2-2-011 (S), RG 148/19 (S)); iGrant of Singapore (A2083c0053).

Acknowledgments. The research of the project was in part supported by Ministry of Education, Singapore, under grant AcRF TIER 1 2019-T1-002-050 (RG 148/19 (S)). The research of the project was also supported by Ministry of Education, Singapore, under grant AcRF TIER 2 (MOE2018-T2-2-011 (S)). This work is also supported by National Research Foundation of Singapore through the Competitive Research Program (NRF-CRP19-2017-01). This work is also supported by National Research Foundation of Singapore through the NRF-ANR Joint Grant (NRF2018-NRF-ANR009 TIGER). This work is also supported by the iGrant of Singapore A*STAR AME IRG (A2083c0053). The authors would like to acknowledge and thank the Nanyang NanoFabrication Centre (N2FC).

Disclosures. The authors declare no conflicts of interest.

References

1. J. Liu, X. Sun, D. Pan, X. Wang, L. C. Kimerling, T. L. Koch, and J. Michel, "Tensile-strained, n-type Ge as a gain medium for monolithic laser integration on Si," Opt. Express **15**(18), 11272–11277 (2007).
2. F. Zhang, V. H. Crespi, and P. Zhang, "Prediction that uniaxial tension along <111> produces a direct band gap in germanium," Phys. Rev. Lett. **102**(15), 156401 (2009).
3. G. Capellini, G. Kozlowski, Y. Yamamoto, M. Lisker, C. Wenger, G. Niu, P. Zaumseil, B. Tillack, A. Ghrib, M. de Kersauson, M. El Kurdi, P. Boucaud, and T. Schroeder, "Strain analysis in SiN/Ge microstructures obtained via Si-complementary metal oxide semiconductor compatible approach," J. Appl. Phys. **113**(1), 013513 (2013).
4. M. J. Süess, R. Geiger, R. A. Minamisawa, G. Schiefler, J. Frigerio, D. Chrastina, G. Isella, R. Spolenak, J. Faist, and H. Sigg, "Analysis of enhanced light emission from highly strained germanium microbridges," Nat. Photonics **7**(6), 466–472 (2013).
5. D. Nam, D. S. Sukhdeo, J.-H. Kang, J. Petykiewicz, J. H. Lee, W. S. Jung, J. Vučković, M. L. Brongersma, and K. C. Saraswat, "Strain-induced pseudoheterostructure nanowires confining carriers at room temperature with nanoscale-tunable band profiles," Nano Lett. **13**(7), 3118–3123 (2013).
6. G.-E. Chang and H. H. Cheng, "Optical gain of germanium infrared lasers on different crystal orientations," J. Phys. D: Appl. Phys. **46**(6), 065103 (2013).
7. D. S. Sukhdeo, D. Nam, J.-H. Kang, M. L. Brongersma, and K. C. Saraswat, "Direct bandgap germanium-on-silicon inferred from 5.7% (100) uniaxial tensile strain," Photonics Res. **2**(3), A8 (2014).
8. A. Ghrib, M. El Kurdi, M. Prost, S. Green, X. Checoury, G. Beaudoin, M. Chaigneau, R. Ossikovski, I. Sagnes, and P. Boucaud, "All-around SiN stressor for high and homogeneous tensile strain in germanium microdisk cavities," Adv. Opt. Mater. **3**(3), 353–358 (2015).
9. A. Z. Al-Attili, S. Kako, M. K. Husain, F. Y. Gardes, N. Higashitarumizu, S. Iwamoto, Y. Arakawa, Y. Ishikawa, H. Arimoto, K. Oda, T. Ido, and S. Saito, "Whispering gallery mode resonances from Ge micro-disks on suspended beams," Front. Mater. **2**(43), 1–9 (2015).
10. D. S. Sukhdeo, D. Nam, J.-H. Kang, M. L. Brongersma, and K. C. Saraswat, "Bandgap-customizable germanium using lithographically determined biaxial tensile strain for silicon-compatible optoelectronics," Opt. Express **23**(13), 16740–16749 (2015).
11. A. Gassenq, S. Tardif, K. Guilloy, G. Osvaldo Dias, N. Pauc, I. Duchemin, D. Rouchon, J. M. Hartmann, J. Widiez, J. Escalante, Y. M. Niquet, R. Geiger, T. Zabel, H. Sigg, J. Faist, A. Chelnokov, F. Rieutord, V. Reboud, and V. Calvo, "Accurate strain measurements in highly strained Ge microbridges," Appl. Phys. Lett. **108**(24), 241902 (2016).
12. K. Guilloy, N. Pauc, A. Gassenq, Y. M. Niquet, J. M. Escalante, I. Duchemin, S. Tardif, G. Osvaldo Dias, D. Rouchon, J. Widiez, J. M. Hartmann, R. Geiger, T. Zabel, H. Sigg, J. Faist, A. Chelnokov, V. Reboud, and V. Calvo, "Germanium under high tensile stress: nonlinear dependence of direct band gap vs strain," ACS Photonics **3**(10), 1907–1911 (2016).
13. P. H. Lim, S. Park, Y. Ishikawa, and K. Wada, "Enhanced direct bandgap emission in germanium by micromechanical strain engineering," Opt. Express **17**(18), 16358–16365 (2009).
14. R. W. Millar, K. Gallacher, J. Frigerio, A. Ballabio, A. Bashir, I. Maclaren, G. Isella, and D. J. Paul, "Analysis of Ge micro-cavities with in-plane tensile strains above 2%," Opt. Express **24**(5), 4365–4374 (2016).
15. J. Petykiewicz, D. Nam, D. S. Sukhdeo, S. Gupta, S. Buckley, A. Y. Piggott, J. Vučković, and K. C. Saraswat, "Direct bandgap light emission from strained germanium nanowires coupled with high-Q nanophotonic cavities," Nano Lett. **16**(4), 2168–2173 (2016).

Optics EXPRESS

16. D. Burt, A. Al-Attili, Z. Li, F. Gardès, M. Sotto, N. Higashitarumizu, Y. Ishikawa, K. Oda, O. M. Querin, S. Saito, and R. Kelsall, "Enhanced light emission from improved homogeneity in biaxially suspended Germanium membranes from curvature optimization," Opt. Express **25**(19), 22911–22922 (2017).
17. D. Burt, J. Gonzales, A. Al-Attili, H. Rutt, A. Z. Khokar, K. Oda, F. Gardes, and S. Saito, "Comparison of uniaxial and polyaxial suspended germanium bridges in terms of mechanical stress and thermal management towards a CMOS compatible light source," Opt. Express **27**(26), 37846–37858 (2019).
18. J. Liu, X. Sun, R. Camacho-Aguilera, L. C. Kimerling, and J. Michel, "Ge-on-Si laser operating at room temperature," Opt. Lett. **35**(5), 679–681 (2010).
19. R. E. Camacho-Aguilera, Y. Cai, N. Patel, J. T. Bessette, M. Romagnoli, L. C. Kimerling, and J. Michel, "An electrically pumped germanium laser," Opt. Express **20**(10), 11316–11320 (2012).
20. M. El Kurdi, H. Bertin, E. Martincic, M. De Kersauson, G. Fishman, S. Sauvage, A. Bosseboeuf, and P. Boucaud, "Control of direct band gap emission of bulk germanium by mechanical tensile strain," Appl. Phys. Lett. **96**(4), 041909 (2010).
21. J. R. Sánchez-pérez, C. Boztug, F. Chen, F. F. Sudradjat, D. M. Paskiewicz, R. B. Jacobson, M. G. Lagally, and R. Paiella, "Direct-bandgap light-emitting germanium in tensilely strained nanomembranes," Proc. Natl. Acad. Sci. U. S. A. **108**(47), 18893–18898 (2011).
22. D. Nam, D. Sukhdeo, A. Roy, K. Balram, S.-L. Cheng, K. C.-Y. Huang, Z. Yuan, M. Brongersma, Y. Nishi, D. Miller, and K. Saraswat, "Strained germanium thin film membrane on silicon substrate for optoelectronics," Opt. Express **19**(27), 25866–25872 (2011).
23. M. de Kersauson, M. El Kurdi, S. David, X. Checoury, G. Fishman, S. Sauvage, R. Jakomin, G. Beaudoin, I. Sagnes, and P. Boucaud, "Optical gain in single tensile-strained germanium photonic wire," Opt. Express **19**(19), 17925–17934 (2011).
24. A. Ghrib, M. El Kurdi, M. de Kersauson, M. Prost, S. Sauvage, X. Checoury, G. Beaudoin, I. Sagnes, and P. Boucaud, "Tensile-strained germanium microdisks," Appl. Phys. Lett. **102**(22), 221112 (2013).
25. V. Reboud, A. Gassenq, K. Guilloy, G. O. Osvaldo Dias, J. M. Escalante, S. Tardif, N. Pauc, J. M. Hartmann, J. Widiez, E. Gomez, E. B. Amalric, D. Fowler, D. Rouchon, I. Duchemin, Y. M. Niquet, F. Rieutord, J. Faist, R. Geiger, T. Zabel, E. Marin, H. Sigg, A. Chelnokov, and V. Calvo, "Ultra-high amplified strain on 200 mm optical Germanium-On-Insulator (GeOI) substrates: towards CMOS compatible Ge lasers," Proc. SPIE **9752**, 97520F (2016).
26. A. Gassenq, K. Guilloy, G. Osvaldo Dias, N. Pauc, D. Rouchon, J.-M. Hartmann, J. Widiez, S. Tardif, F. Rieutord, J. Escalante, I. Duchemin, Y.-M. Niquet, R. Geiger, T. Zabel, H. Sigg, J. Faist, A. Chelnokov, V. Reboud, and V. Calvo, "1.9% bi-axial tensile strain in thick germanium suspended membranes fabricated in optical germanium-on-insulator substrates for laser applications," Appl. Phys. Lett. **107**(19), 191904 (2015).
27. R. A. Minamisawa, M. J. Süess, R. Spolenak, J. Faist, C. David, J. Gobrecht, K. K. Bourdelle, and H. Sigg, "Top-down fabricated silicon nanowires under tensile elastic strain up to 4.5%," Nat. Commun. **3**(1), 1096 (2012).
28. S. Bao, D. Kim, C. Onwukaeme, S. Gupta, K. Saraswat, K. H. Lee, Y. Kim, D. Min, Y. Jung, H. Qiu, H. Wang, E. A. Fitzgerald, C. S. Tan, and D. Nam, "Low-threshold optically pumped lasing in highly strained germanium nanowires," Nat. Commun. **8**(1), 1–7 (2017).
29. F. T. Armand Pilon, A. Lyasota, Y. M. Niquet, V. Reboud, V. Calvo, N. Pauc, J. Widiez, C. Bonzon, J. M. Hartmann, A. Chelnokov, J. Faist, and H. Sigg, "Lasing in strained germanium microbridges," Nat. Commun. **10**(1), 2724 (2019).
30. H. T. Tong, N. Nishiharaguchi, T. Suzuki, and Y. Ohishi, "Mid-infrared transmission by a tellurite hollow core optical fiber," Opt. Express **27**(21), 30576–30588 (2019).
31. M. El Kurdi, M. Prost, A. Ghrib, S. Sauvage, X. Checoury, G. Beaudoin, I. Sagnes, G. Picardi, R. Ossikovski, and P. Boucaud, "Direct band gap germanium microdisks obtained with silicon nitride stressor layers," ACS Photonics **3**(3), 443–448 (2016).
32. A. Elbaz, M. El Kurdi, A. Aassime, S. Sauvage, X. Checoury, I. Sagnes, C. Baudot, F. Boeuf, and P. Boucaud, "Germanium microlasers on metallic pedestals," APL photonics **3**(10), 106102 (2018).
33. G. Capellini, C. Reich, S. Guha, Y. Yamamoto, M. Lisker, M. Virgilio, A. Ghrib, M. El Kurdi, P. Boucaud, B. Tillack, and T. Schroeder, "Tensile Ge microstructures for lasing fabricated by means of a silicon complementary metal-oxide-semiconductor process," Opt. Express **22**(1), 399–410 (2014).
34. Y. Ishikawa, K. Wada, D. D. Cannon, J. Liu, H.-C. Luan, and L. C. Kimerling, "Strain-induced band gap shrinkage in Ge grown on Si substrate," Appl. Phys. Lett. **82**(13), 2044–2046 (2003).
35. R. Geiger, T. Zabel, E. Marin, A. Gassenq, J.-M. Hartmann, J. Widiez, J. Escalante, K. Guilloy, N. Pauc, D. Rouchon, G. O. Diaz, S. Tardif, F. Rieutord, I. Duchemin, Y.-M. Niquet, V. Reboud, V. Calvo, A. Chelnokov, J. Faist, and H. Sigg, "Uniaxially stressed germanium with fundamental direct band gap," 1, (2015).
36. I. H. Jafri, H. Busta, and S. T. Walsh, "Critical point drying and cleaning for MEMS technology," *Proc. SPIE*, 3880 (1999).
37. Y. P. Varshini, "Temperature dependence of bandgap," Physica **34**(1), 149–154 (1967).
38. B. Dutt, D. S. Sukhdeo, D. Nam, B. M. Vulovic, Z. Yuan, and K. C. Saraswat, "Roadmap to an efficient germanium-on-silicon laser: strain vs. n-type doping," IEEE Photonics J. **4**(5), 2002–2009 (2012).
39. D. Nam, D. S. Sukhdeo, S. Gupta, J. Kang, M. L. Brongersma, and K. C. Saraswat, "Study of carrier statistics in uniaxially strained Ge for a low-threshold Ge laser," IEEE J. Sel. Top. Quantum Electron. **20**(4), 16–22 (2014).